NUREG/IA-0236

International Agreement Report

Analysis and Computational Predictions of CHF Position and Post-CHF Heat Transfer

Prepared by:
B. Belhouachi, S.P. Walker, G.F. Hewitt

Nuclear Research Group
Mechanical Engineering Department
Imperial College
London SW7 2BX
UK

A. Calvo, NRC Project Manager

Office of Nuclear Regulatory Research
U.S. Nuclear Regulatory Commission
Washington, DC 20555-0001

May 2010

Prepared as part of
The Agreement on Research Participation and Technical Exchange
Under the Thermal-Hydraulic Code Applications and Maintenance Program (CAMP)

Published by
U.S. Nuclear Regulatory Commission

AVAILABILITY OF REFERENCE MATERIALS IN NRC PUBLICATIONS

NRC Reference Material

As of November 1999, you may electronically access NUREG-series publications and other NRC records at NRC's Public Electronic Reading Room at http://www.nrc.gov/reading-rm.html. Publicly released records include, to name a few, NUREG-series publications; *Federal Register* notices; applicant, licensee, and vendor documents and correspondence; NRC correspondence and internal memoranda; bulletins and information notices; inspection and investigative reports; licensee event reports; and Commission papers and their attachments.

NRC publications in the NUREG series, NRC regulations, and *Title 10, Energy*, in the Code of *Federal Regulations* may also be purchased from one of these two sources.

1. The Superintendent of Documents
   U.S. Government Printing Office
   Mail Stop SSOP
   Washington, DC 20402–0001
   Internet: bookstore.gpo.gov
   Telephone: 202-512-1800
   Fax: 202-512-2250
2. The National Technical Information Service
   Springfield, VA 22161–0002
   www.ntis.gov
   1–800–553–6847 or, locally, 703–605–6000

A single copy of each NRC draft report for comment is available free, to the extent of supply, upon written request as follows:

Address: Office of the Chief Information Officer,
Reproduction and Distribution
Services Section
U.S. Nuclear Regulatory Commission
Washington, DC 20555-0001
E-mail: DISTRIBUTION@nrc.gov
Facsimile: 301–415–2289

Some publications in the NUREG series that are posted at NRC's Web site address http://www.nrc.gov/reading-rm/doc-collections/nuregs are updated periodically and may differ from the last printed version. Although references to material found on a Web site bear the date the material was accessed, the material available on the date cited may subsequently be removed from the site.

Non-NRC Reference Material

Documents available from public and special technical libraries include all open literature items, such as books, journal articles, and transactions, *Federal Register* notices, Federal and State legislation, and congressional reports. Such documents as theses, dissertations, foreign reports and translations, and non-NRC conference proceedings may be purchased from their sponsoring organization.

Copies of industry codes and standards used in a substantive manner in the NRC regulatory process are maintained at—

The NRC Technical Library
Two White Flint North
11545 Rockville Pike
Rockville, MD 20852–2738

These standards are available in the library for reference use by the public. Codes and standards are usually copyrighted and may be purchased from the originating organization or, if they are American National Standards, from—

American National Standards Institute
11 West 42nd Street
New York, NY 10036–8002
www.ansi.org
212–642–4900

Legally binding regulatory requirements are stated only in laws; NRC regulations; licenses, including technical specifications; or orders, not in NUREG-series publications. The views expressed in contractor-prepared publications in this series are not necessarily those of the NRC.

The NUREG series comprises (1) technical and administrative reports and books prepared by the staff (NUREG–XXXX) or agency contractors (NUREG/CR–XXXX), (2) proceedings of conferences (NUREG/CP–XXXX), (3) reports resulting from international agreements (NUREG/IA–XXXX), (4) brochures (NUREG/BR–XXXX), and (5) compilations of legal decisions and orders of the Commission and Atomic and Safety Licensing Boards and of Directors' decisions under Section 2.206 of NRC's regulations (NUREG–0750).

DISCLAIMER: This report was prepared as an account of work sponsored by an agency of the U.S. Government. Neither the U.S. Government nor any agency thereof, nor any employee, makes any warranty, expressed or implied, or assumes any legal liability or responsibility for any third party's use, or the results of such use, of any information, apparatus, product, or process disclosed in this publication, or represents that its use by such third party would not infringe privately owned rights.

ABSTRACT

The objective of the current study is to investigate the capability of the US NRC TRACE code to predict the Critical Heat Flux (CHF) position and temperature profiles for different axial heat flux distributions in the reflooding of a hot single tube. Measurements of each of Bennett, Keeys and Becker were used for this.

Hydrodynamic and post-dryout heat transfer calculations were performed using TRACE Code. CHF and critical quality correlations (based on the 'look-up' tables of Groeneveld, the 'local conditions' hypothesis, and the boiling length/quality relationship) are usually implemented in system codes. Each of these has been used to analyze the experiments. These simulations showed that generally the CHF position was well predicted whereas the estimation of the wall temperature was not correct for particular ranges of mass and heat fluxes. This is investigated and possible causes, associated with 'local conditions' issues, are proposed.

FOREWORD

This document reports an investigation of the US NRC TRACE code in regards to the prediction of the Critical Heat Flux (CHF) position and temperature profiles for different axial heat flux distributions in the reflooding of a hot single tube.
We outline strengths and deficiencies of the reflood module of the TRACE system code. In fact, we perform a simulation for a single tube where initial and boundary conditions are in the range of Large Break Loss-of-Coolant-Accident conditions.
Conclusions imply a better modeling of the reflooding for both tubes, and by extension for rod bundles.

CONTENTS

Page

Abstract iii

Foreword v

List of Figures viii

Executive Summary ix

Acknowledgement x

Abbreviations xi

1. Introduction 1-1

2. Critical heat flux and post dryout heat transfer 2-1
- 2.1 Critical Heat Flux (CHF) Prediction Methods 2-1
- 2.2 Dispersed Flow Film Boiling (DFFB) 2-2
- 2.3 Experiments 2-4

3. Simulations 3-1
- 3.1 TRACE 3-1
- 3.2 Nodalization and Fine Mesh Technique 3-1
- 3.3 Simulations, results and comparisons 3-2

4. Conclusions 4-1

5. References 5-1

LIST OF FIGURES

Page

Fig. 1 Nodalization study 3-1

Fig. 2 CHF position and temperature predictions for a uniform heat flux 3-3

Fig. 3 CHF position and temperature predictions for a non-uniform heat flux 3-3

Fig. 4 Effect of pressure on dryout position 3-4

Fig. 5 Dryout position and temperature profiles 3-5

Fig. 6 Comparison between calculated and experimental temperature profiles 3-5

Fig. 7 Effect of wall friction factor on temperature distribution 3-6

Fig. 8 Influence of the droplet drag on the temperature profile prediction 3-7

Fig. 9 Comparison of different heat transfer correlations 3-7

Fig. 10 Assessment of a proposed model 3-9

EXECUTIVE SUMMARY

The analysis and the assessment of the TRACE codes demonstrate its ability to well predict the point of critical heat flux reasonably well. However, the temperature profile, and thus, the peak clad temperature, is not well predicted for the case of a non-uniform heat flux. For the case of uniform heat flux distributions, the combination of the so-called ‘Look-Up Tables’ and the Biasi critical quality provides results that match well with the Bennett experimental data. This is not true at high mass and heat fluxes.

The study of the DFFB models usually implemented in thermal-hydraulics system code such as TRACE established the crucial character of the interfacial heat transfer. A key point would be to study the variations of the heat transfer coefficient and its sensitiveness to both the mentioned correlations and the interfacial area concentration (which has not been treated in this paper for simplicity). The droplet drag did not play an important role in the calculations performed here. The two-phase enhancement factor applied in the wall heat transfer correlation, namely, the Gnielinski correlation, had a little influence on the temperature predicted for the experiments simulated. The droplet diameter and the number density are important in the prediction of both the position of dryout and the temperature profile upstream from the quench front (precursory cooling effects).

ACKNOWLEDGEMENT

The authors would like to acknowledge EPSRC for the funding under grant EP/C549465/1, the UK - HSE and the US NRC for making available the TRACE code.

ABBREVIATIONS

AECL	Atomic Energy of Canada Limited, Canada
AFD	Axial-heat Flux Distribution
CHF	Critical Heat Flux
DFFB	Dispersed Flow Film Boiling
IPPE	Institute of Power and Physics, Obninsk-Russia
LWR	Light Water Reactor
NRC	Nuclear Regulatory Commission, USA
PCT	Peak Clad Temperature

NOMENCLATURE

	Nomenclature
B	Blowing factor
c_p	Specific heat (J/kg-K)
C_D	Drag coefficient
D	Diameter
D_H	Hydraulic diameter (m)
F	Friction factor
g	Gravitational acceleration (m/s^2)
G	Mass flux (kg/m^2-s)
Gr	Grashof no.
k	Conductivity
K	Dummy factor
L_B	Boiling Length (m)
Nu	Nusselt no.
P	Pressure (Pa)
Pr	Prandt no.
q''	Heat flux (W/m^3)
Re	Reynolds no.
T	Temperature
V	Velocity (m/s)
x	Quality

	Greek symbols
α	Void fraction
β	Exponent
μ	Viscosity
ρ	density
$\Psi_{2\Phi}$	Two-Phase enhancement factor

	Subscripts
CHF	Related to CHF
$conv$	Related to convection
d	Related to droplet
FC	Related to forced convection
g	Related to gas
l	Related to liquid
lam	Related to laminar flow
rad	Related to radiation
sat	Related to saturation
$turb$	Related to turbulent flow
v	Related to vapour
w	Related to wall

1. INTRODUCTION

The integrity of the cladding of the nuclear fuel of Light Water Reactors (LWR) as first containment barrier is of high importance in nuclear safety. The cladding is intended to operate with a temperature less than 2200°F (~1477°K) to avoid both oxidation and radial expansion. The situations for which such a temperature can be reached are numerous. A typical description is the presence of a blanket of vapour surrounding the pin inducing a very sharp decrease in heat transfer and consequent temperature increase.

While the design intent is generally to avoid this condition, predicting the Peak Clad Temperature (PCT) is important. Geometric factors and operating parameters (pressure, power profiles, mass flow rates, inlet sub-cooling to name a few) affecting the Critical Heat Flux (CHF), the maximum heat flux applied to a solid surface for which unstable vapour patches appear, have been investigated in the past [1-3] and resulted in many correlations.

Hence, it has become increasingly difficult to select the correct CHF prediction methods that can be used for a variety of conditions and geometries. Additionally, a lack of knowledge of the undergoing heat transfer regimes encountered in the post-CHF region has limited the development of theoretical models.

This present work intends to first provide a study of the main correlations implemented in system codes, (such as the 1995 Groeneveld look-up table [1], the Biasi and CISE-GE correlations). A focus will be on the quench front (CHF location with a wall superheat of about 200°K [2]) and the temperature profiles in the Dispersed Flow Film Boiling (DFFB) region. The computer code used as a basis for these simulations is the thermal-hydraulics system code TRACE, developed by the US NRC. A feature of the TRACE code, the fine mesh technique, was used in order to gain in accuracy; we will investigate this issue.

Along these same lines, the above-mentioned CHF prediction methods will be assessed in the case of uniform and cosine axial-heat flux distributions (AFD) for a range of pressures and mass fluxes in tubes.

In a second part, we will discuss the modelling of the post-CHF heat transfer and the sensitivity of the code to the different correlations accounting for the interfacial droplet drag, the interfacial heat transfer and the wall heat transfer.

Finally, we have performed some calculations with a selected set of post-dryout heat transfer correlations where a ‘Blowing’ factor accounting for the effect of the mass transfer upon the heat transfer was added to the interfacial droplet drag and the interfacial heat transfer. A two-phase enhancement factor, which represents the enhancement of the convective heat transfer in the expression of the wall-to-gas heat flux due to the presence of the dispersed droplets in the superheated vapour flow, is commonly implemented and tuned in system codes to fit data. In here, we will conserve its original form and study its influence on the de-superheating of the vapour phase.

2. Critical Heat Flux and Post Dryout Heat Transfer

2.1 Critical Heat Flux (CHF) prediction methods

As noted, the critical heat flux (CHF) is the heat flux for which a heated surface becomes vapour-blanketed with increasing heat flux inputs. The vapour patches/blanket resulting from this excess in heat flux leads to a deterioration of the convective heat transfer exchanges between the wall and the coolant. The superheat beyond the CHF point could significantly be of the order of 600°K.

In general, three approaches are adopted in the prediction of the CHF:

- The 1995 AECL[1]-IPPE[2] "look-up" tables [1],
- Flux-quality relationships, and
- Boiling length/quality relationships.

The differences between the two latter relationships are reported in [3].

It is usually accepted that the Groeneveld look-up tables comply with the margin requirements imposed by both nuclear regulatory bodies and energy producers. However, the main assumption is that CHF can be determined on local conditions basis, i.e.:

$$\dot{q}''_{CHF} = K \cdot fn\left\{P, G, x, D_H\right\} \tag{1}$$

where $\dot{q}''_{CHF}$ is the critical heat flux, *K* is a product of factors accounting for the geometry, low flow conditions etc. *P* is the pressure, *G* the mass flux, *x* the quality and D_H is the hydraulic diameter. From Eq. (1), it could be understood that the Groeneveld et al. tables [1] imply a specific relationship between CHF and local quality for a given mass flux and pressure. Nevertheless, the relationship between heat flux ($\dot{q}''_{CHF}$) and quality (*x*) is not a universal one and this is amply proved by data for non-uniform heat flux, exemplified by some Refrigerant-114 data from Shiralkar [4].

The two other approaches, namely the *F*-factor and the boiling length approaches, allow better results to be obtained.

The *F*-factor method developed by Tong et al. [5] takes into account the influence of the non-uniformity of the heat flux upon the prediction of the CHF. The so-called *F*-factor is defined at a given enthalpy as the ratio of a uniform heat flux (CHF) to the non-uniform CHF. As this approach assumes the importance of the effect of the upstream heat flux profile on the local CHF, it has to be noted that at low qualities, the 'memory effect' is small, and thus the CHF is conditioned by the local heat flux. At high qualities, this same 'memory effect' is sizeable and the average heat flux fixes the CHF position.

On the other hand, the boiling length/ critical quality (x_{CHF}) relationship introduced by Bertoletti et al. [6] is expressed as:

$$x_{CHF} = K_i \frac{A \cdot L_B}{B + L_B} \tag{2}$$

where L_B is the boiling length, i.e. the distance from which the fluid reaches saturation, *x=0*; K_i is a factor accounting for the radial peaking factor and, in the case of the Biasi correlation,

1 AECL: Atomic Energy of Canada Limited.

2 IPPE: Institute of Power and Physics, Obninsk, Russia.

accounting for the ratio between the heated perimeter to the wetted perimeter. '*A'* and '*B'* are two system-dependent functions, i.e.: $A = fn\{P, G\}$ and $B = fn\{P, G, D_H\}$.

In the TRACE code, the CHF position is essentially determined by the 1995 look-up tables (notwithstanding the non-physical nature of the local condition hypothesis). The reason is that the overall average and the RMS errors associated with the adoption of this approach are 0.38% and 8.17% respectively, which in practice, is difficult to better. In addition to this prediction method, the user can combine the prediction of the CHF with the CISE-GE [7] or Biasi [8] critical quality correlation. The critical quality value is only used as a transition criterion from pre to post-CHF while the CHF point ($\dot{q}''_{CHF}, T_{CHF}$) remains determined by the Groeneveld et al. tables [9]. No attempt was made to modify the determination of the CHF point by other means than the look-up tables.
In part 2, we present results of the effect of the different correlations described above on the temperature distribution.

2.2 Dispersed Flow Film Boiling (DFFB)

The regimes present in the post-CHF region are the inverted annular flow and/or the dispersed flow film boiling (dispersed droplet mixture in a superheated continuous vapour phase). Here we discuss only the latter given the high void fractions $\alpha \geq 0.80$ encountered above the dryout location. The modelling of DFFB heat transfer is, in computer codes, a three step process: wall-vapour heat transfer, vapour-drop convection, and wall to drop heat transfer.

2.2.1 Wall heat transfer

The wall heat transfer is a combination of forced convection to the superheated vapour and thermal radiation to the liquid droplets.
Therefore, the heat flux is expressed as follow:

$$q''_{DFFB} = q''_{wg,FC} + q''_{wg,rad} + q''_{wl,rad} + q''_{wd} \tag{3}$$

The wall temperature is often greater than the Leidenfrost temperature, the droplet-to-wall[3] contact could be considered by an enhanced Forslund-Rohsenow correlation at high vapour Reynolds no. ($Re_v \geq 4000$):

$$h_{dw} = 0.00638(Re_v - 4000)^{0.6}(1-\alpha)^{2/3}\left[\frac{k_v h_{fg} g \rho_d \rho_v}{(T_w - T_d)\mu_g D_d}\right]^{0.25} \tag{4}$$

The convective wall-to-gas heat transfer ($q''_{wg,FC}$) is usually calculated by making the key assumption that the heat transfer is similar to single-phase forced convection heat transfer. A correction factor ($\Psi_{2\Phi}$), which accounts for the two-phase heat transfer exchanges enhancement due to the presence of the dispersed droplets in the continuous vapour phase, is added to the Gnielinski[4] correlation [10]:

3 In highly turbulent flows (and at high pressure), the droplet radial velocity increases, therefore, droplets-wall interactions should not be neglected since they participate to the rewetting hot walls.

4 At the moderate Reynolds nos. entrance length effects can enhance the wall heat transfer but are neglected in this present study.

$$q''_{wg,FC} = \frac{k_g}{D_H} \cdot Nu_{wg,FC} \cdot \Psi_{2\Phi} \cdot (T_w - T_l) \tag{5}$$

where:

$$Nu_{wg,FC} = \begin{cases} Nu_{lam} = 4,36 \\ Nu_{turb} = \dfrac{(f/2)(Re-1000)\cdot Pr}{1+12.7\cdot(f/2)^{1/2}\cdot(Pr^{2/3}-1)} \end{cases} \tag{6}$$

In Eq. (6) *f* is a friction factor, and:

$$\Psi_{2\Phi} = \left[1 + \frac{(1-\alpha)\cdot g \cdot \Delta\rho \cdot D_H}{2\cdot f_w \cdot \rho_g \cdot V_g^2}\right]^{1/2} \tag{7}$$

f_w is the wall friction factor and V_g is the gas velocity.

In general, the axial gradient of vapour superheat first increases and then, due to the precursory cooling effects, decreases with increasing axial distance downstream from the quench front.
The effect of heat transfer on the vaporization of the liquid phase could be caused by either heat transfer from the superheated vapour to the entrained liquid or from heat transfer from the superheated wall to the liquid.
Hence, the interfacial heat transfer between the vapour phase and the droplet mixture plays a key role in determining the maximum superheat of the vapour, which in turn limits the Peak Clad Temperature (PCT). We will discuss this point in the next section.

2.2.2 Drop drag and interfacial heat transfer

The modelling of the dispersed phase requires a particular attention in regard to the interfacial droplet drag and the interfacial heat transfer. A critique of the key assumptions in the modelling of DFFB regimes in multiphase flow system codes can be found in [11].
We will only mention the assumptions relevant to our analysis.
First, for the calculation of both interfacial drag and heat transfer, it is assumed that the cloud of droplets of a range of sizes can be represented by a single representative[5] spherical (justified by small Eotvos no.) droplet with the same area to volume ratio as that of the entire population.
The physical mechanisms that affect the droplet size distribution (impingement on the wall, evaporation, break-up, coalescence) are ignored. The droplet size is taken to depend only on local conditions, namely relative velocity and fluid properties and is calculated from the local critical Weber no. Thus, the number density of droplets generated at the locus of CHF varies in the computational domain whereas this transport of the droplet population should be history-dependent and consistent.
Droplet-to-droplet interactions are incorporated through empirical approximations. In TRACE, for example, this is accomplished through the evaluation of an empirical correlation based on the local flow conditions and is calculated using the correlation of Kataoka, Ishii and Mishima [12].
In some other computer codes, the recent trend of multi-field modelling intends to solve this problem [13].

Moreover, since the droplets are mainly generated at the quench front where the fluid properties are at saturation, the droplet temperature is expected to be at saturation (no

5 This representation is limited, in fact, a same volume may produce different interfacial.

conduction/convection inside the drop). Only heat transfer exchanges on the vapour side are considered. Then, the interfacial heat transfer coefficient could be based either on the Lee and Ryley correlation developed at atmospheric pressure:

$$Nu_d = 2 + 0.74\,\mathrm{Re}^{1/2}\,\mathrm{Pr}_v^{1/3} \tag{8}$$

Or on the correlation suggested by Ranz and Marshall [14]:

$$Nu_d = 2 + 0.60\,\mathrm{Re}^{1/2}\,\mathrm{Pr}_v^{1/3} \tag{9}$$

The drag coefficient is expressed as:

$$C_D = \frac{24}{Re_d} \cdot (1 + 0.1 \cdot Re_d^{0.75}) \tag{10}$$

Studies on the sensitivity of the temperature distribution to different drag coefficients and interfacial heat transfer correlations are presented in the results section. The main modification is the addition of the so-called 'Blowing factor' accounting for the effect of mass transfer upon heat transfer in the expressions of drag coefficient and Nusselt no.

2.3 Experiments

From the experimental studies available in the literature, we have selected the Bennett et al. [15] data set for uniformly heated tube. To investigate the effect of the axial heat flux distribution, we use the Keeys et al. [16] tests for which a cosine heat flux distribution was applied to a tube. Thirdly, the Becker et al. [17] study on the post dryout heat transfer which, for instance, reveals the importance of pressure on the dryout location, has been modelled.

The objective of the Bennett experiment was essentially to obtain a measure of the wall surface temperature in the region beyond the dryout point. The dryout 'interface' between the heated wall and the dry regions was investigated and has led to the demonstration of the non-equilibrium effects associated with developing flows in heated tubes. The variables reported were the mass flux, system pressure, wall heat flux, inlet sub-cooling and quality. Systematic experiments in a 12.6 mm internal diameter tube were conducted at the constant pressure of 6.89MPa. At a given mass flow rate, the heat flux was varied by an increment of ~1%, and the axial temperature profiles measured.

In another UKAEA study, Keeys et al. in 1971 examined the post-CHF heat transfer in a 3.66m long tube with a cosine heat flux distribution (with a form factor of 1.4). The data set are summarized in table 1. These two experiments demonstrated the dependency of the local critical heat flux on the axial heat flux distribution. In fact, at the same dryout quality, the CHFs of the non-uniformly heated tube were noticeably lower than those measured on the uniformly heated tubes. Hence the necessity of modelling the post dryout heat transfer in a non-uniform heated tube by taking into account the flow history, in other terms: the boiling length.

Becker et al. [17] conducted at the Royal Institute of Technology (RIT) in Stockholm post dryout experiments where the wall temperatures were measured on a set of 7 m long electrically heated tubes with inner diameters of 10, 14.9 and 24.7 mm. The tube was cooled by upwards flow of water with mass fluxes from 500 to 3000 kg/m2-s. However, in this present work, the cases selected covered pressures ranging from 3 to 14MPa, heat fluxes from 400 to 1060kW/m^2 and inlet sub-cooling from 8.5 to 12K.

Table 1: Experimental data

Year	**Experiment**	**P (MPa)**	**G (Kg/m^{2}s)**	**D (mm)**	**L (m)**	**X**	**Q (MW/m^2)**

1967	Bennett	6.9	393-5235	12.6	5.56	-	0.35-1.84
1972	Keeys	6.9	700-4100	12.7	3.66	0.15-0.95	0.8-1.5
1983	Becker	3-20	500-3000	14.9	7.0	0.03-1.60	0.1-1.25

3. Simulations

3.1 TRACE (TRAC-RELAP Advance Computational Engine)

TRACE is a thermal-hydraulics computational modelling code for nuclear power systems developed by the US Nuclear Regulatory Commission (US-NRC). TRACE is a code designed to analyze reactor transients and accidents up to the point of fuel failure. The partial differential equations that describe the two-phase flow and heat transfer are solved using the finite volume numerical methods. The heat-transfer equations are evaluated using a semi-implicit time-differencing technique while the Navier-Stokes equations in the spatial one-dimensional (1D) and three-dimensional (3D) components use, by default, a multi-step time-differencing procedure that allows the material Courant-limit condition to be exceeded. In this present paper, all results presented arise from one dimensional modelling.

3.2 Nodalization and Fine Mesh Technique

Nodalization studies with shorter test section cells show that decreasing the length from 0.30 m to 0.10 m did not noticeably increase the accuracy in predictions as illustrated in figure 1. CHF and temperature profile predictions require correct numerical and physical models. The approach adopted by developers is to improve the numerical techniques implemented in two-fluid codes such as TRACE in order to track both the variations of the void fraction (level tracking methods) and the thermal gradient at the quench front (fine mesh rezoning techniques) [9].

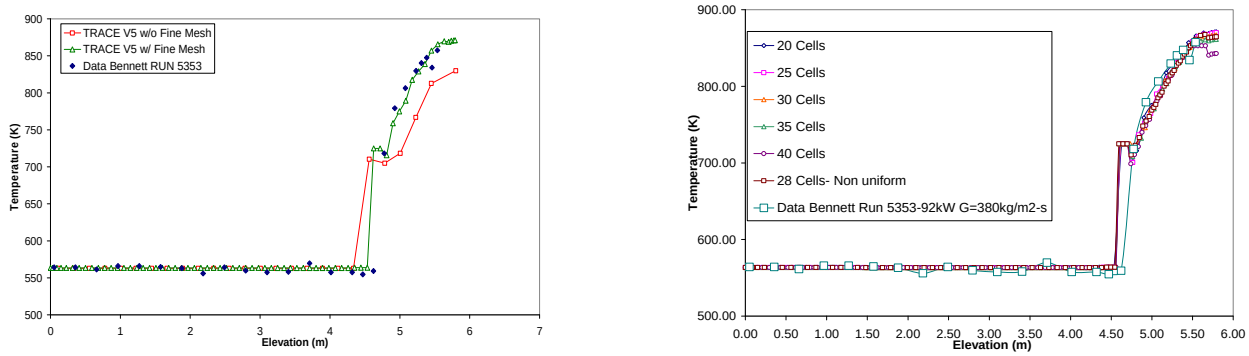

Figure 1. Nodalization study for the Bennett run 5353, on the left, the case was run with the fine mesh technique activated. On the right, the nodalization shows that a number of 20 cells is sufficient.

With a fine mesh technique, the axial resolution of the axial gradient involves the insertion of transitory nodes whenever the difference between adjacent nodes exceeds a heat transfer regime dependent value ΔT_{max}, usually of the order of 25°C. The figure 2-c, modelling the Bennett run 5358, shows indeed a good agreement, the predictions fit perfectly the data at low mass fluxes and low heat fluxes while using the Biasi correlation. The analysis of the output reveals that even though the last part of the graph tends to be similar, the heat transfer regimes are different: we encounter the DFFB in the run performed with the fine mesh technique and single phase vapour heat transfer in the other.

A maximum number of 1000 transitory nodes and a minimum distance of 1 mm between two adjacent nodes were imposed. These criteria suggest that the technique is consistent with the space-averaging theory on which is based the two-fluid formulation [18]. In the selected data, the regimes are liquid and vapour single phase, nucleate boiling, transition boiling and DFFB. With a drop size lower than 1 mm, we are assuming that the fine mesh technique is suitable for

DFFB. According to this preliminary study, most of runs were performed using this fine mesh technique, generally used in transient and quasi-steady reflood-like situations.
However, those calculations failed to predict well the position of the CHF and the temperature profile in the dryout region; at this stage, one could question the validity of the physical models implemented in system codes. The precursory cooling effects (due to slugs and droplets generated at the quench front) could be important beyond the CHF; this phenomenon controls the wall temperature by essentially cooling down the superheated vapour. Recent work in this area has been carried out by Andreani and Yadigaroglu [19-21] and contributed to a better understanding of the physics involved in the post-dryout region.
Also, the wall-droplet interactions could be significant, but they are usually not modelled. In fact, the wall temperature in the DFFB regime is often above the temperature at which a droplet will wet the wall (the Leidenfrost point). The recent strategy to tackle this physical problem is to implement a multi-field model [22, 23] and to have a better treatment of the interfacial area by solving the interfacial area transport equation [24-26] coupled to a macroscopic $k-\varepsilon$ model [27].

3.3 Simulations, results and comparisons

The code assessment process is based on the comparison between the computed predictions and experimental data in order to validate individual physical models. In this paper, we are interested in the prediction of the critical heat flux position but also in the interfacial droplet drag, interfacial heat transfer and wall heat transfer in the post dryout region. In the following results, we have added when necessary a Blowing factor *B* to account for the evaporation process. In fact, the drag dependency on the mass efflux (evaporation or condensation) is real and proved. In TRACE, the model of Renksizbulut and Yuen [28] is attended to re-transcribe the effect of mass transfer upon heat transfer.

3.3.1 CHF and critical quality correlations

The determination of the CHF location is crucial and determines the extent of the temperature rise in the post-CHF region. As mentioned earlier, we used here the different options available in the TRACE code:

- AECL-IPPE (Look-Up Tables),
- AECL-IPPE with the Biasi critical quality correlation,
- AECL-IPPE with the CISE-GE critical quality correlation.

The latter was developed for rod-bundle geometries and is not expected to provide the best fit to data. Moreover, the correlation is adequate only for mass fluxes in the range: $300 \le G \le 1400$ (kg/m^2-s). On the contrary, the Biasi correlation developed for tubes is stated to be valid for mass fluxes in the range: $100 \le G \le 6000$ (kg/m^2-s); we recall here that the Biasi correlation was corrected to account for the conversion from ATA to Bar units [29]. Again, using the Bennett run 5359, the comparison (Figure 2-d) establishes that both the look-up table method and the Biasi critical quality predict satisfactorily the data. However, the simulation of a Keeys test at high power and high mass flux shows that none of the correlation predicts the dryout point. The CISE-GE correlation is the best prediction for this particular run despite the fact that it was primarily developed for rod bundle geometries.
As the Biasi critical correlation is based on the boiling length approach essentially accounting for the history of the flow upstream from the dryout point, it was used for our simulations.

An important step in the code assessment process is to check whether TRACE is capable of estimating the dryout point for uniform and non uniform heat flux distributions. Figure 2

demonstrates that TRACE is able to predict well the CHF location and the temperature profile for a uniform heat flux at low mass flux ($G = 380 kg / m^2 s$) for different heat inputs.

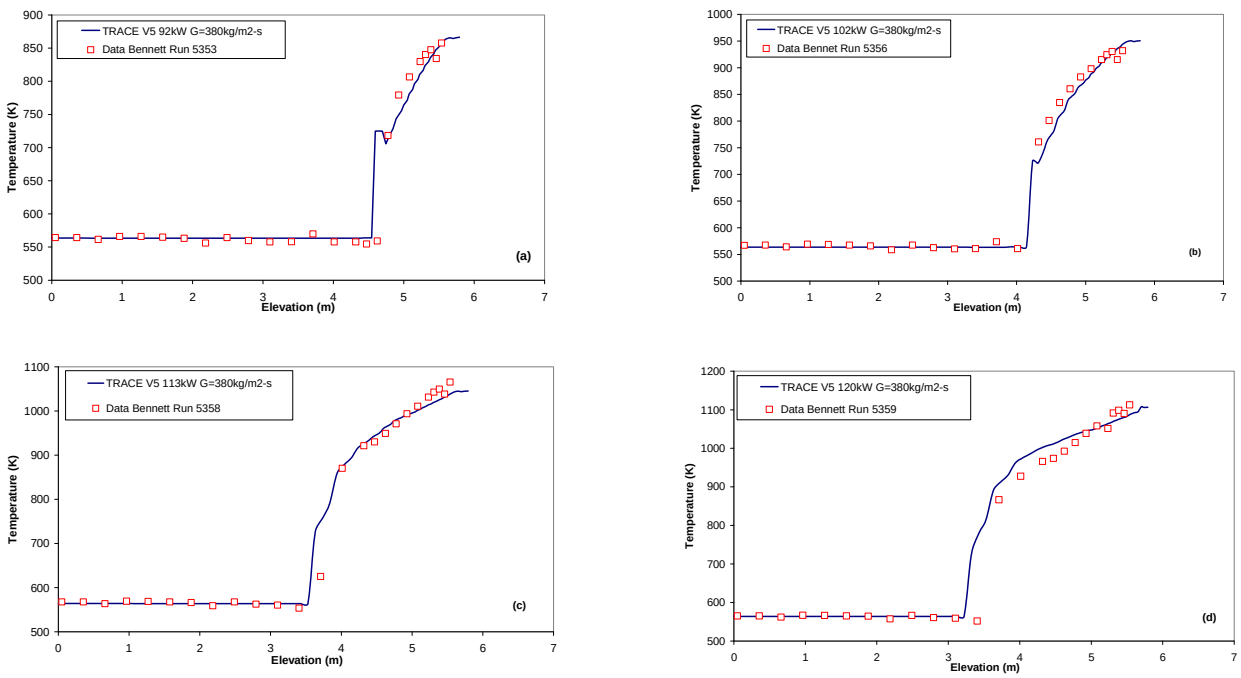

Figure 2. CHF position and temperature predictions for a uniform heat flux (Bennett Data).

In the case of non-uniform heat flux, the prediction is less good. Indeed, we notice on figure 3-b that the position of dryout is over-predicted by about 0.6m.

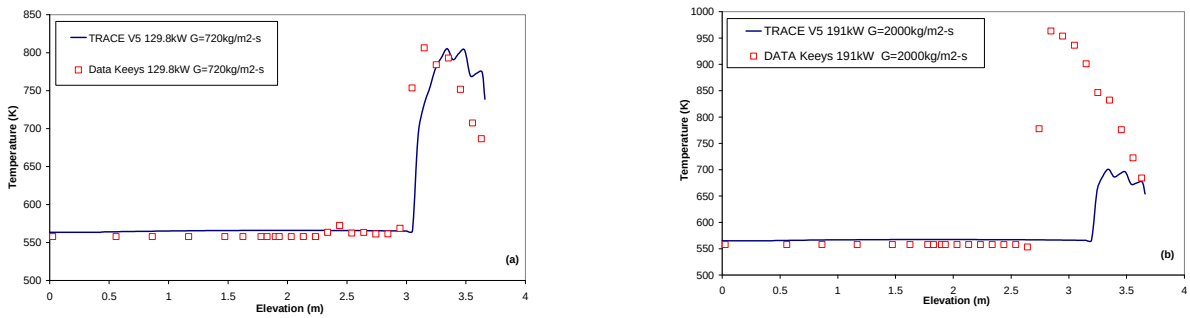

Figure 3. CHF position and temperature predictions for a non-uniform heat flux (Keeys data).

The pressure also influences the prediction of the dryout point and the consequent post dryout heat transfer exchanges. At constant mass flux and power input, an increasing pressure favours the occurrence of CHF; the predictions of the Becker tests confirm this behaviour (figure 4). Downstream from the dryout point, the temperatures appear to tend to an asymptotic value. This could be explained by the fact that in this region, only vapour exists and some sort of equilibrium homogenises the thermal exchanges.

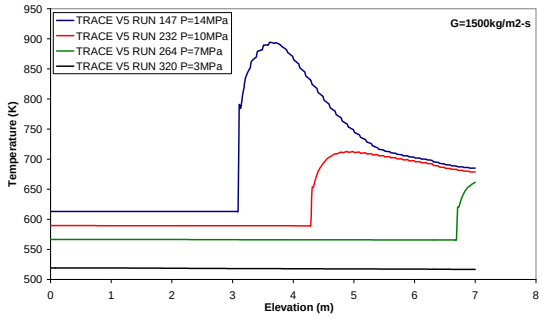

Figure 4. Effect of pressure on the dryout position at a constant mass flux of 1500kg/m^2-s and at a constant heat flux of 760kW/m^2 (Becker data).

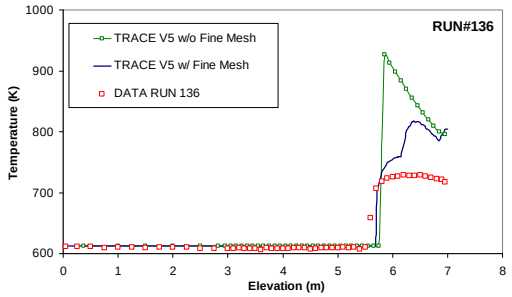

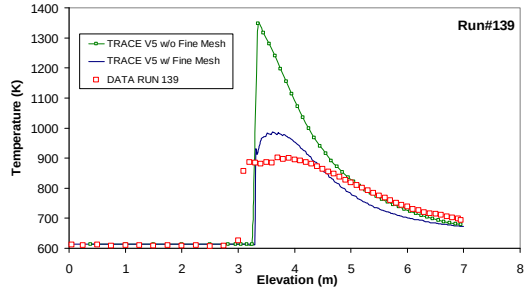

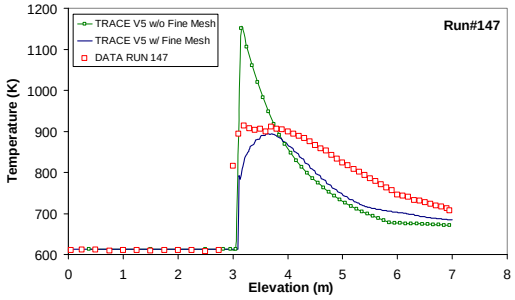

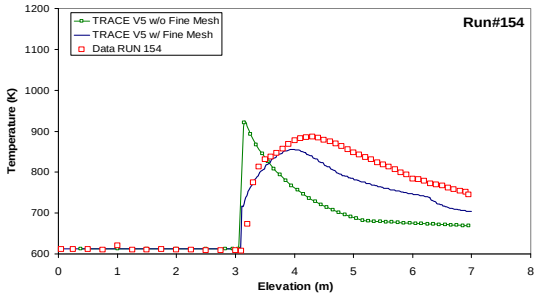

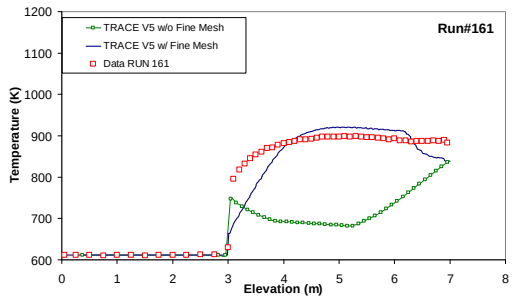

Figure 5. Dryout position and temperature profiles for the calculations of the Becker tests at constant pressure (14MPa) and varying mass fluxes (from the top left corner to the right bottom corner: 1977, 1970, 1494, 1006, 503 kg/m^2-s).

In short, these previous results demonstrate the ability of the code to predict the CHF location and post-dryout heat transfer reasonably well at low mass fluxes and low uniform heat fluxes using the Groeneveld et al. [1] 'look-up tables' with the Biasi critical quality correlation. Indeed, in Figure 5 and 6, one can notice that at high heat fluxes and high mass fluxes, the CHF is still well predicted but the distribution of temperatures is now less well predicted. Also, at a given heat flux and pressure, and for conditions of low mass velocities, the code fails to estimate either the CHF position and/or the temperature profile. It is worth noting that when the CHF position is forced by the authors to occur at a given elevation (Figure 6-b), the temperature distribution beyond the dryout point does not coincide with experimental data and the PCT is under-predicted. Indeed, two reasons could be suggested, (1) non-equilibrium effects become significant and hence the reduction in accuracy and (2) upstream history effects are predominant in the development of film boiling.
Since the CHF point was, in most cases, well estimated; we decided to focus on the DFFB regime by implementing modified and/or new models into the thermal-hydraulics TRACE code.

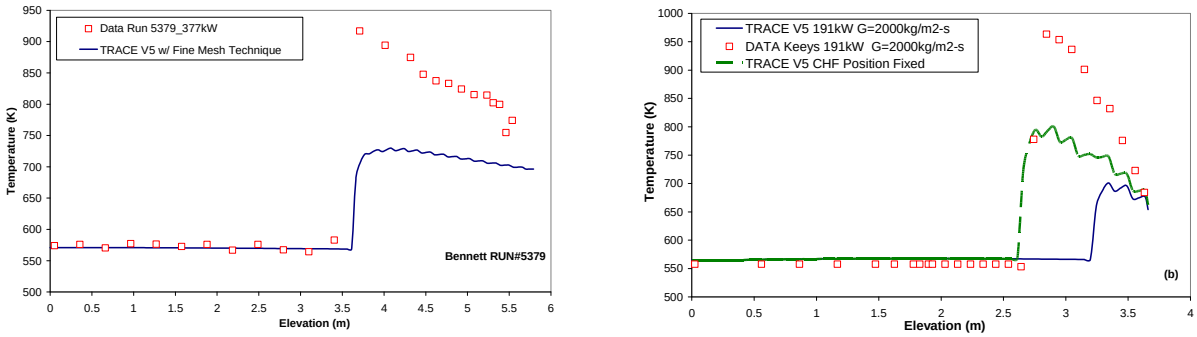

Figure 6. Comparison between calculated temperature profiles and: (left) the Bennett experimental run 5379 (P=6.9MPa, G=3800kg/m^2-s and Power=377kW); (right) the Keeys data (P=6.9MPa, G=2000kg/m^2-s and Power=191kW) while the computed CHF position is fixed

3.3.2 Two-phase enhancement factor

In this section, the two-phase enhancement factor ($\Psi_{2\Phi}$) is used in the following form:

$$\Psi_{2\Phi} = 1 + K_{\Psi} \cdot \left[\frac{(1-\alpha) \cdot Gr_{2\Phi}}{Re_g^2} \right]^n \tag{11}$$

where $Gr_{2\Phi}$ is the Grashof no. ($Gr_{2\Phi} = (\rho_g \cdot g \cdot \Delta\rho \cdot D_H^3 / \mu_g^3)$), K_{Ψ} is a wall friction factor dependant coefficient ($2 \le K_{\Psi} \le 100$) and the exponent *n* takes either the value of 0.5 or 0.85 depending on the droplet diameter considered. While K_{Ψ} is too high, the two-phase enhancement factor becomes important in Eq. (5) causing a higher heat flux and then under-predicting the PCT. However, as it could be noticed in figure 7, the TRACE is not sensitive to a change of values for K_{Ψ} .

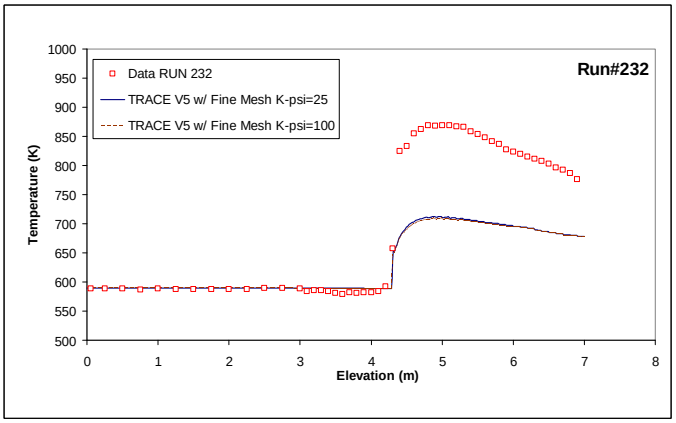

Figure 7. Effect of different K_{Ψ} values on the temperature distribution for the Becker run 232 (P=10MPa and G=1500kg/m^2-s)

3.3.3 Interfacial Droplet Drag

As mentioned in part 2, the evaluation of droplet drag is crucial. This encouraged us to investigate the impact of different correlations on post-CHF regimes. For conditions of constant relative velocity, the droplet drag C_D is related to the droplet Reynolds no. as follow:

$$\begin{aligned} 0 < Re_d < 2 \qquad & C_D = 24 / Re_d \\ 2 \le Re_d < 500 \quad & C_D = 0.4 + 40 / Re_d \\ 500 \le Re_d \le 10^5 \qquad & C_D = 0.44 \end{aligned} \tag{12}$$

As an alternative to the expression of the droplet drag C_D in Eq.(10), we used a drag law which has been obtained in the context of an accelerating cloud of droplets; Ingebo [30] has studied particle acceleration and has correlated a wide range of data by the expression:

$$C_D = \frac{27}{Re_d^{0.84}} \tag{13}$$

Indeed, a model for accelerating cloud of droplets is likely better to represent the physics involved. Thermal gradients can cause the continuous vapour phase to be accelerated increasing the droplet mean velocity.

In order to account for the effect of evaporation on the drag coefficient, a factor has been added to the previous expression:

$$C_D^{new} = \frac{C_D}{(1+B)^{0.2}} \tag{14}$$

where the blowing factor *B* suggested by Renksizbulut and Yuen [28] is:

$$B = \left(\frac{c_{P,g} \cdot (T_g - T_{sat})}{h_{fg}} \right) \cdot \left(1 - \frac{q''_{wd}}{q''_{wg}} + \frac{q''_{rad}}{q''_{conv}} \right) \approx \left(\frac{c_{P,g} \cdot (T_g - T_{sat})}{h_{fg}} \right) \tag{15}$$

From the calculations performed (figure 8), one can state that the droplet drag coefficient does not have a significant effect on the PCT. The addition of a blowing factor increases the PCT by no more than 5°K.

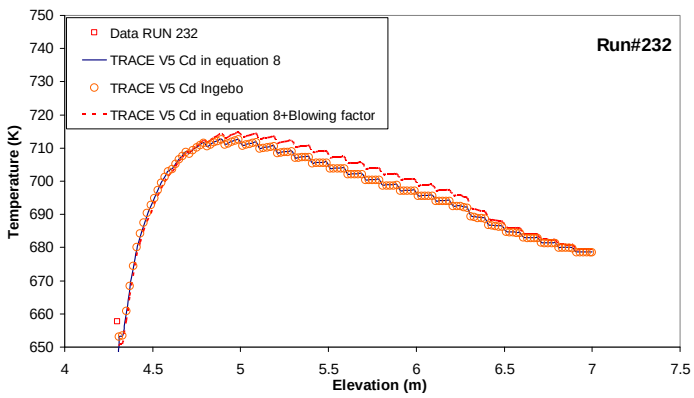

Figure 8. Influence of the droplet drag on the temperature profile prediction for the Becker Run 232 (P=10MPa and G=1500kg/m^2-s).

3.3.4 Interfacial Heat Transfer

Despite the minor effect of the blowing factor on the droplet drag coefficient (figure 8) and therefore on the temperature distribution; figure 9 reveals the central role of the single particle Nusselt no. in the temperature and CHF predictions. The Renksizbulut and Yuen correlation is the correlation implemented in the TRACE code. We have implemented few more correlations (Ranz-Marshall, Lee and Ryley and Beard and Pruppacher) to quantify their respective influences.

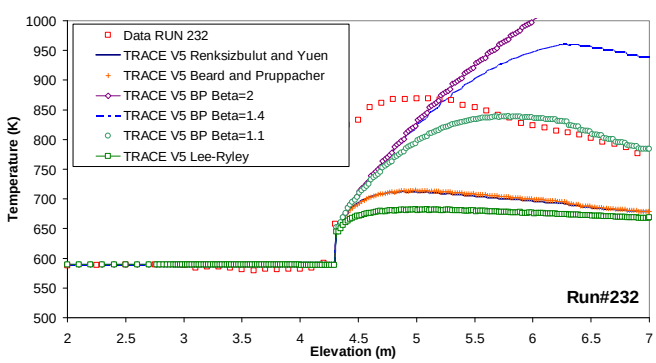

Figure 9. Comparison of different interfacial heat transfer correlations in the DFFB region for the Becker Run 232 (P=10MPa and G=1500kg/m^2-s).

The results obtained with the different correlations show that the best agreement was obtained with a modified version of the Beard and Pruppacher (BP) correlation[31] to account for the mass evaporation:

$$Nu_d = \frac{1.56 + 0.616 Re_d^{1/2} Pr_g^{1/3}}{(1+B)^{\beta}} \tag{16}$$

where $0.07 < \beta < 2.79$.

Eq. (16) determines the single-particle Nusselt no. In our calculations, a multi-particle Nusselt no. is used; this latter contains an additional factor dependant on the void fraction.

The use of the Beard and Pruppacher correlation with a value of 1.1 for the exponent β does not predict the first temperature peak well; but, upstream from the quench front, the precursory cooling effects seem to be well estimated. It is worth noting that the validity of the above correlations can be discussed in the sense that most of them were obtained at atmospheric pressure and at relatively low Reynolds nos.

3.3.5 A selected set of constitutive laws for heated single tubes

In this section, we have chosen a set of correlations which (1) better suited the conditions of the Bennett, Keeys and Becker experiments and (2) accounted for more physical phenomena (3) enables us to over-predict the PCT (measure of safety). The graphs (figure 10) were obtained while expressing the interfacial droplet drag from a modified version of the Schiller-Naumann correlation accounting for the mass efflux:

$$C_D = \frac{24}{Re_d} \cdot \frac{(1 + 0.15 \cdot Re_d^{0.687})}{(1+B)^{0.2}} \qquad 0 \le Re_d \le 1000 \tag{17}$$

However, we select the maximum value of the drag in between the latter, 0.44 and the Ingebo drag coefficient value.

The interfacial heat transfer was based on the Beard and Pruppacher correlation:

$$Nu_d = \frac{1.56 + 0.616 Re_d^{1/2} Pr_g^{1/3}}{(1+B)^{1.1}} \tag{18}$$

and the two-phase enhancement factor considers a wall friction factor value for a smooth pipe of 0.005:

$$\Psi_{2\Phi} = 1 + 100 \cdot \left[\frac{(1-\alpha) \cdot Gr_{2\Phi}}{Re_g^2} \right]^{1/2} \tag{19}$$

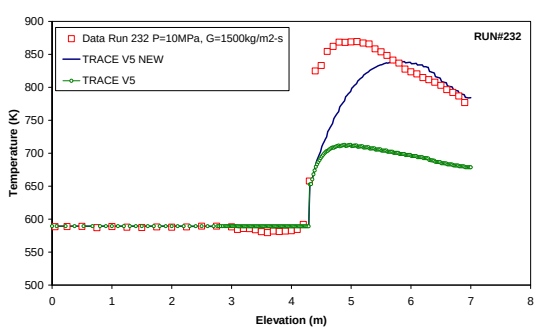

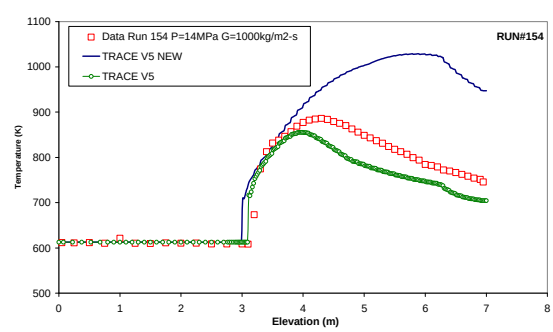

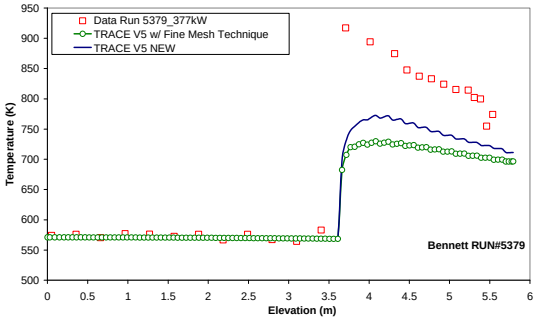

Figure 10. Assessment of the proposed model for the Becker Run 232 (top left) and 154 (top right): the over-prediction of the temperature is due to poor precursory cooling effects. In this model, there is too rapid evaporation of the droplets beyond the dryout point leading to single phase vapour convection, with the vapour not cooled further by the dispersed droplets. As for the Bennett run (bottom), the temperature is slightly higher but not high enough to fit the data.

In our modelling, we do not account for the droplet-to-wall heat transfer or for radiation. This set of correlations (Eq.(17), (18),(19)) is supposed to better represent the physics involved such as the droplet mass evaporation, droplet drag coefficient derived from accelerating cloud of droplets etc. Nevertheless, some results (figure 10) exhibited large discrepancies right after the CHF point. The calculation of both the droplet diameter (at a critical Weber number value of 12) and the relative velocity might cause these differences. A too high relative velocity value induces an under-prediction of the temperature at low mass flux.
Regarding the Blowing factor, the mass efflux from the droplet reduces the convective heat transfer from the superheated steam: the evaporation process increases the boundary layer thickness leading to a sharp decrease in heat transfer to the droplet surface, which in return reduces the rate at which additional mass can be added. This shielding effect is limited in our calculations and droplets completely evaporate.

4. Conclusion

The analysis and the assessment of the TRACE codes demonstrate its ability to well predict the point of critical heat flux reasonably well. However, the temperature profile, and thus, the peak clad temperature, is not well predicted for the case of a non-uniform heat flux. For the case of uniform heat flux distributions, the combination of the so-called ‘Look-Up Tables’ and the Biasi critical quality provides results that match well with the Bennett experimental data. This is not true at high mass and heat fluxes.

The study of the DFFB models usually implemented in thermal-hydraulics system code such as TRACE established the crucial character of the interfacial heat transfer. A key point would be to study the variations of the heat transfer coefficient and its sensitiveness to both the mentioned correlations and the interfacial area concentration (which has not been treated in this paper for simplicity). The droplet drag did not play an important role in the calculations performed here. The two-phase enhancement factor applied in the wall heat transfer correlation, namely, the Gnielinski correlation, had a little influence on the temperature predicted for the experiments simulated. The droplet diameter and the number density are important in the prediction of both the position of dryout and the temperature profile upstream from the quench front (precursory cooling effects).

5. REFERENCES

[1] Groeneveld, D.C., L.K.H. Leung, P.L. Kirillov, V.P. Bobkov, I.P. Smogalev, V.N. Vinogradov, X.C. Huang, and E. Royer," The 1995 look-up table for critical heat flux in tubes", *Nuclear Engineering and Design* Vol. 163, No. 1-2, 1996, pp. 1-23.

[2] Evans, D., S. Webb, and J.C. Chen," Axially varying vapor superheats in convective film boiling", *ASME Journal of Heat Transfer* Vol. 107, 1985, pp. Pages: 663-669.

[3] Yang, J., D.C. Groeneveld, L.K.H. Leung, S.C. Cheng, and M.A.E. Nakla," An experimental and analytical study of the effect of axial power profile on CHF", *Nuclear Engineering and Design* Vol. 236, No. 13, 2006, pp. 1384-1395.

[4] Shiralkar, B.S.," Analysis of non-uniform CHF data in simple geometries", *Report NEDM-13279*, 1972.

[5] Tong, L.S.," Prediction of departure from nucleate boiling for an axially non-uniform heat flux distribution", *Journal of Nuclear Energy* Vol. 21, No. 3, 1967, pp. 241-248.

[6] Bertoletti, S., G.P. Gaspari, C. Lombardi, G. Peterlongo, M. Silvestri, and F.A. Tacconi," Heat transfer crisis with steam-water mixtures", *Energia Nucl. (Milan); Vol: 12*, 1965, pp. Pages: 121-172.

[7] Borkowski, J.A., N.L. Wade, S.Z. Rouhani, R.W. Shumway, W.L. Weaver, W.H. Rettig, and C.L. Kullberg, "TRAC-BF1/MOD1 models and correlations", 1992, pp. Size: 449 p.

[8] Biasi, L., G.C. Clerici, S. Garribba, R. Sala, and A. Tozzi," Studies on burnout. Part 3. A new correlation for round ducts and uniform heating and its comparison with world data", *Energ. Nucl. (Milan), 14: 530-6(Sept. 1967).* 1967.

[9] US-NRC, "TRACE V5.0 Theory Manual", 2007.

[10] Gnielinski, V.," New equations for heat and mass transfer in turbulent pipe and channel flow", *Int. Chem. Eng.*, 1976, pp. pp. 359–368.

[11] Andreani, M., and G. Yadigaroglu, "Dispersed Flow Film Boiling", 1992.

[12] Kataoka, I., M. Ishii, and K. Mishima," Generation and size distribution of droplet in annular two-phase flow", *J. Fluids Eng. ; Vol/Issue: 105*, 1983, pp. Pages: 230-238.

[13] Jayanti, S., and M. Valette," Prediction of dryout and post-dryout heat transfer at high pressures using a one-dimensional three-fluid model", *International Journal of Heat and Mass Transfer* Vol. 47, No. 22, 2004, pp. 4895-4910.

[14] Ranz, W.E., and W.R. Marshall," Evaporation from drops. Parts I & II", *Chemical Engineering Progress* Vol. 48:141-6; 173-80, 1952.

[15] Bennett, A.W., G.F. Hewitt, H.A. Kearsey, and R.K.F. Keeys, "Heat transfer to steam-water mixtures flowing in uniformly heated tubes in which the critical heat flux has been exceeded", *Technical report AERE-R5373*, 1967.

[16] Keeys, R.K.F., J.C. Ralph, and D.N. Roberts, "Post burnout heat transfer in high pressure steam water mixtures in a tube with cosine heat flux distribution", 1971, pp. Size: Pages: 69.

[17] Becker, K.M., C.H. Ling, S. Hedberg, and G. Strand," An experimental investigation of post-dryout heat tansfer", *Report KTH-NEL-33, Royal Institute of Technology, Stockholm, Sweden*, 1983.

[18] Pasamehmetoglu, K.O., and R.A. Nelson, "Investigation of the quasi-steady approach used in transient two-phase flow analysis", United States, 1988, pp. Pages: 24.

[19] Andreani, M., and G. Yadigaroglu," Prediction methods for dispersed flow film boiling", *International Journal of Multiphase Flow* Vol. 20, No. Sup, 1994, pp. 1.

[20] Andreani, M., and G. Yadigaroglu," A 3-D Eulerian-Lagrangian Model of Dispersed Flow Film Boiling -II. Assesment Using Quasi-Steady-State Data and Comparison with Results of 1-D Analyses", *Int. J. Heat Mass Transfer* Vol. 40, No. 8, 1997, pp. 1773-1793.

[21] Andreani, M., and G. Yadigaroglu," A 3-D Eulerian-Lagrangian model of dispersed flow film boiling including a mechanistic description of the droplet spectrum evolution - I. The thermal-hydraulic model", *International Journal of Heat and Mass Transfer* Vol. 40, No. 8, 1997, pp. 1753-1772.
[22] Kawaji, M., and S. Banerjee," Application of a multifield model to reflooding of a hot vertical tube: Part 1 - Model structure and interfacial phenomena", *Journal of Heat Transfer (Transcations of the ASME (American Society of Mechanical Engineers), Series C) ; Vol/Issue: 109:1*, 1987, pp. Pages: 204-211.
[23] Kawaji, M., and S. Banerjee," Application of a multifield model to reflooding of a hot vertical tube: Part 2 - Analysis of experimental results", *Journal of Heat Transfer (Transcations of the ASME (American Society of Mechanical Engineers), Series C) ; Vol/Issue: 110:3*, 1988, pp. Pages: 710-720.
[24] Sun, X., M. Ishii, and J.M. Kelly," Modified two-fluid model for the two-group interfacial area transport equation", *Annals of Nuclear Energy* Vol. 30, No. 16, 2003, pp. 1601-1622.
[25] Delhaye, J.-M.," Some issues related to the modeling of interfacial areas in gas-liquid flows, II. Modeling the source terms for dispersed flows", *Comptes Rendus de l'Academie des Sciences - Series IIB - Mechanics* Vol. 329, No. 6, 2001, pp. 473-486.
[26] Delhaye, J.-M.," Some issues related to the modeling of interfacial areas in gas-liquid flows I. The conceptual issues", *Comptes Rendus de l'Academie des Sciences - Series IIB - Mechanics* Vol. 329, No. 5, 2001, pp. 397-410.
[27] Serre, G., and D. Bestion, "Progress in improving two-fluid model in system code using turbulence and interfacial area equations", *NURETH-11*, 2005.
[28] Renksizbulut, M., and M.C. Yuen," Experimental study of droplet evaporation in a high-temperature air stream", *J. Heat Transfer ; Vol/Issue: 105*, 1983, pp. pp. 384–388.
[29] Todd, D.R., and H. Tang," Application of the Biasi CHF Correlation: Purposeful Interpretation or Historical Accident?" *ASME*, 2007.
[30] Ingebo, R.D.," Drag coeficients for droplets and solid spheres in clouds accelerating in air streams", *NACO - Technical Note 3762*, 1956.
[31] Beard, K.V., and H.R. Pruppacher," A wind tunnel investigation of collection kernels for small water drops in air", *Q. J. R. Meteorol. Soc.* Vol. Volume 97, 1971, pp. pp. 242–248.